Available online at www.sciencedirect.com
SCIENCE DIRECT
Remote Sensing of Environment 102 (2006) 318–327
Remote Sensing of Environment
www.elsevier.com/locate/rse

Assessing spatial patterns of forest fuel using AVIRIS data

Gensuo J. Jia [a,b,*], Ingrid C. Burke [a], Alexander F.H. Goetz [c], Merrill R. Kaufmann [d], Bruce C. Kindel [c]

[a] Department of Forest, Rangeland, and Watershed Stewardship, and Natural Resource Ecology Laboratory, Colorado State University, Fort Collins, CO 80523, USA
[b] RCE-TEA, Institute of Atmospheric Physics, Chinese Academy of Sciences, Beijing 100029, China
[c] Center for the Study of Earth from Space, University of Colorado, Boulder, CO 80309, USA
[d] Rocky Mountain Research Station, USDA Forest Service, Fort Collins, CO 80526, USA

Received 18 August 2005; received in revised form 2 February 2006; accepted 18 February 2006

Abstract

Montane coniferous forests and woodlands in the Front Range of the Colorado Rocky Mountains have been subject to increased wildfire in recent years. The area and intensity of these fires is strongly dependent upon the spatial variability and type of fuels as they are arrayed across the landscape. Considering the size of the patches and the mosaic of fuel materials, high spectral and spatial resolution estimates of vegetation components and fuel types are needed to improve fire risk assessment, especially around the wildland/urban interface. Here we used highly resolved remotely sensed imagery, in combination with several spectral techniques to map major forest components and fuel types in montane coniferous forests in the Colorado Front Range by discriminating the fractional covers of photosynthetic vegetation (PV), non-photosynthetic vegetation (NPV) and bare soil at a sub-pixel level. An accuracy assessment based on a dataset including 34 field transects indicated that we could explain fractional cover of 73.5%, 40.3%, and 77.6% for PV, NPV, and soil respectively through the use of hyperspectral indicators. Based on the fractional cover of these components, we were able to assess the spatial patterns of vegetation and fuel characteristics at a landscape scale. Throughout the study areas, PV fractions were dominant (48.7%), followed by NPV (28.8%) and soil (22.5%). However, due to microclimate and disturbances such as fire, insect infestations and forest management practices, the spatial distribution of fractions was highly heterogeneous. There was a high fraction of PV in mature forest and on north-facing slopes, and a high fraction of NPV and bare soil in areas with recent disturbance such as fire or insect infestation. In severely burned areas, bare soil was dominant. Fuel treatments reduced the fraction of PV by 11.7%, and increased fractions of NPV by 7.4% and bare soil by 4.5%. These results suggest that hyperspectral remote sensing can be an excellent indicator of not only fuel fractional cover, but of fuel condition after fire, thereby greatly improving regional fire risk assessment.

Keywords: Fire; Fuel; Spectral mixture analysis; Conifer forest; Colorado Front Range

1. Introduction

Wildland fires have become intense and more frequent during the past decade in the western U.S. states (Brown et al., 2004) as a result of maturing second-growth forests, climatic change (Fried et al., 2004), and long-term fire suppression (Keeley et al., 1999). Many of these fires were in the wildland/urban interface, and so caused severe property damage and threatened human life (Schoennagel et al., 2004). Meanwhile, large scale severe forest fires also strongly influence vegetation structure (Dwire & Kauffman, 2003; Laughlin et al., 2004), forest productivity (Keane et al., 1990), ecosystem carbon storage (Law et al., 2003; Lynch & Wu, 2000), and increase the chance of soil erosion (Pierce et al., 2004) and exotic species invasion (Fornwalt et al., 2003). Clearly, it is very important to develop accurate ways to assess fuel characteristics and predict the probability of fires occurring in heterogeneous landscapes (Mast et al., 1998), such as in the Colorado Front Range, so as to prioritize areas for most efficient fuel treatments along wildland/urban interfaces.

Many forest characteristics determine the spatial distribution of fuels and the potential for severe fire, including green canopy

* Corresponding author. Tel.: +1 970 4910495; fax: +1 970 4916754.
E-mail address: jiong@virginia.edu (G.J. Jia).

0034-4257/$ - see front matter © 2006 Elsevier Inc. All rights reserved.
doi:10.1016/j.rse.2006.02.025

closure, vegetation moisture, horizontal and vertical biomass distribution, the ratio of live to dead plant materials, and the distribution of bare ground (Andersen et al., 2005; Dennison et al., 2003; Romme, 1982; Scott & Reinhardt, 2001). The spatial patterns of these characteristics are fundamental information for fire potential assessment and fire behavior modeling (Keane et al., 1990; Miller & Urban, 2000; Scott & Reinhardt, 2001) and many of the characteristics have been linked to spatial distribution of green vegetation, dead plant materials, and bare soil (Asner et al., 1998). Airborne and satellite imagery have been used by forest managers and researchers in forest fuel survey and fire risk assessment for decades, and have shown their advantage across extensive remote areas (Bergen et al., 2000; Hyyppa et al., 2000; Roberts et al., 2003). Traditional field forest survey is still important for ground validation and local-scale study, but is extremely labor intensive and difficult to extrapolate accurately over large areas.

At regional to global scales, remotely sensed fuel and fire studies have been focused on deriving fuel moisture (Dennison et al., 2003), estimating total biomass or fuel, and, mapping fire distribution and frequency (Burgan et al., 1998; Justice et al., 2002) using Landsat, MODIS, and AVHRR data. At a local scale, Lidar data have been widely used to analyze vertical forest structure and to estimate fuel variables such as crown bulk density, tree height and basal area (Andersen et al., 2005; Hall et al., 2005; Lefsky et al., 2002). In recent years, imaging spectroscopy or hyperspectral remote sensing have been demonstrated to be useful for the spectral and spatial discrimination of these fire-related vegetation attributes at a sub-pixel level (Roberts et al., 2003; Ustin et al., 2004). Given sufficient spatial resolution and sensor performance, hyperspectral data provide detailed reflectance information of various fuel materials over the 400–2500 nm region and have shown a much higher accuracy than multi-spectral datasets (Green et al., 1998; Hyyppa et al., 2000; Van Wagtendonk et al., 2004). In arid and semi-arid regions, hyperspectral data have provided detailed surface information on fractions of green vegetation, non-photosynthetic vegetation, and bare soil, as well as canopy structure (Asner & Heidebrecht, 2003; Roberts et al., 1993; Ustin et al., 2004) in sparse vegetation. However, this information has been very limited in forest areas and even more limited in fuel analysis.

In this study, we sought to map three major components of forest fuels, photosynthetic vegetation (PV), non-photosynthetic vegetation (NPV) and bare soil using Airborne Visible/Infrared Imaging Spectrometer (AVIRIS) data, validated by field forest transect samplings. Our objective was to answer the following questions: 1) Can these forest materials be discriminated using high spectral resolution data? 2) What are the fuel characteristics and their spatial distribution for areas planned as fuel treatment areas in a National Forest? 3) Finally, how do disturbances such as mechanical thinning and recent fires alter fuel characteristics? These three questions address the potential for hyperspectral remote sensing for predicting fuel distribution as well as analyzing the effectiveness of fuels treatments.

2. Data and methods

2.1. Study sites

The study sites are located in the Pike National Forest in the Colorado Front Range, approximately 40–80 km southwest of the Denver metropolitan area. Elevations in the area vary from 1900 m in the east to 2800 m in the west; above this elevation is the subalpine zone which has a substantially different fire regime, and which we did not study. Vegetation types in the montane region include ponderosa pine (*Pinus ponderosa*) and Douglas-fir (*Pseudotsuga menziesii* var. *glauca*) forest, mixed conifer forest (the above species plus *Pinus contorta*, *Picea pungens*, *Abies lasiocarpa*) forest, woodland dominated by Pinyon pine (*Pinus edulis*) and juniper (*Juniperus scopulorum*), occasional aspen stands (*Populus tremuloides*) and patches of shrub (*Cercocarpus montanum*)/grassland on south-facing slopes. Watersheds within the Pike National Forest serve as major recreation and water supply areas for Denver residents. As a wildland/urban interface, the area also contains about 4000 households, and has been facing increasing human impact, with a relatively large population growth. From 1990 to 2000 the population in the Colorado Front Range increased by 30.3% (Colorado State Demography, 2003, http://dola.colorado.gov/demog/Housing.cfm). In June 2002, the Hayman Fire, centered at Cheesman Lake on the South Platte River, burned 55,750 ha of natural vegetation and destroyed more than 600 structures, costing nearly 40 million dollars (Graham, 2003). Burn severity ranged from severe, with complete crown mortality, to mixed severity with patchy overstory mortality interspersed with less severe understory fire (Graham, 2003; Schoennagel et al., 2004). The Hayman Fire killed most of the above-ground biomass in a 9830-ha area around Cheesman Lake, and left patches of unburned or lightly burned conifer forest in the south-eastern portion of the fire area. Other nearby fires included Buffalo Creek (1996), Hi Meadows (2000), and Schoonover (2002), all of which had large areas of complete or nearly complete overstory mortality. We examined the Hayman, Buffalo Creek, and Hi Meadow fires in the study (Fig. 1).

Much of the area in the Colorado Front Range has similar elevation, soils, and climate to the Hayman fire area; yet the forest structure is very variable within the region due to local variation in environment and a long history of human impacts (Veblen et al., 2000). Logging began in the 1870s, intensive grazing shortly thereafter, and fire suppression during the 20th century (Baker, 1992). Prior to fire suppression, there were three large scale forest fires recorded in 1723, 1851, and 1880 at Cheesman Lake, which created large areas of openings and a mosaic of forests with various canopy cover (Brown et al., 2004; Kaufmann et al., 2001). During most of the 20th century there were no major forest fires in the region, and fuels gradually increased and forest openings declined (Kaufmann et al., 2000). The 1996–2002 fires mentioned above represent the largest burned area during the entire past half century.

As a fire mitigation effort, the U.S. Forest Service (USFS) developed forest fuel treatment projects in the South Platte watershed to systematically reduce fuel loading using prescribed

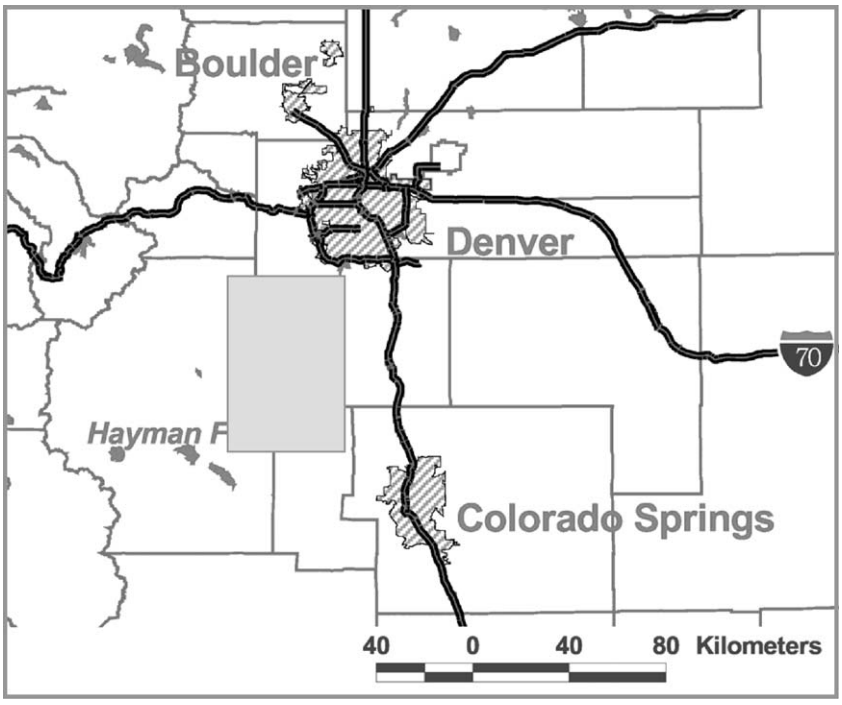

Fig. 1. Location of study area highlighted as grey rectangle.

burning and mechanical thinning. We closely collaborated with USFS managers who were planning and conducting fuel management treatments.

We made field measurements in the study areas in the fall of 2002 and 2003 as part of a NASA funded application study on fire hazard analysis and carbon sequestration. The field measurements included fractional cover of major forest components for canopy and understory, fuel loading of each size class, field spectra of dominant photosynthetic and non-photosynthetic materials, as well as fire severity (Brown et al., 1982; Asner et al., 1998). We established 100 m transects located within relatively homogeneous landscapes in the region. Most importantly for this paper, these data were used to estimate the fractional covers and derive standard field spectra of forest components for validating estimates from AVIRIS data.

2.2. Field measurements of fractional cover

We made field measurements of fractional cover along 34 100-m forest transects randomly selected in our study areas. We generated 246 random points within each of the burned areas, eliminating points with poor accessibility. Burn severity was also considered during sample site selection, to maximize the diversity of sites sampled. Along each 100-m transect, we randomly selected 5 points at approximately 20-m intervals, and used Brown transects (Brown et al., 1982) and modified-Whittaker methods (Stohlgren et al., 1995) for field sampling. At each of the points we laid out a 15-m transect at a randomly selected angle from the original 100-m transect. Along each 15-m sub-transect we measured: 1) complete overstory inventories of tree diameter, height, age, species, live or dead status, and stem mapped tree location; 2) percentage cover of live leaves, live branches, charred branches, scorched branches, and openings of canopy layer using a densiometer; 3) percentage cover of shrub, herbaceous, litter, woody debris, bare soil, and rock on the ground; and 4) evidence of recent fire and burn severity (Omi & Martinson, 2002). For overstory measurements, we counted all small trees (less than 3 m tall) within a 3-m radius from the end point of the 15-m transect, and measured four large trees at the beginning point. We used the 15-m transect line to divide the area around the beginning point into four quadrants. We selected the closest tree in each quadrant that is greater than 3 m tall and measured diameter at breast height (DBH), tree height, height to the first live branch, height of burned parts of the tree, burn severity, bark thickness, and crown width. We used these data to develop regions of interest (ROIs) of various fuel types, to calculate fractional covers of each forest component (PV, NPV, and soil) for ground reference data, and to summarize fuel loading for each sample site.

We used the 2002–2003 transect data to calculate the fractional cover of PV, NPV, and soil. For the canopy layer, we measured percentage cover of live tree crowns, dead tree crowns, and openings. We summarized live tree crowns as PV, dead tree crowns as NPV, and openings as total understory cover. For understory, we measured fractional cover of bare soil (soil), herbaceous (NPV/PV), shrub (PV), rock (soil), woody debris (NPV), and litter (NPV). We then summarized the fractional cover of PV, NPV, and soil for each transect. These field-based fractional cover values were later used to validate our hyperspectral estimates.

2.3. Field spectral reflectance measurements

We acquired field reflectance spectra of plant species and various materials including deadwood, char wood, duff, litter,

bare soil, and rock in late September to mid-October with a FieldSpec Pro spectrometer (Analytical Spectral Devices, Boulder, CO) over the 400–2500 nm wavelength region at 1 nm intervals. We sampled in the fall to coincide with the AVIRIS flight. The measurements were made on cloud-free days between 11:00 and 13:00 to reduce atmospheric contamination and minimize the effects of a change in solar zenith. The spectrometer was positioned approximately 1 m from the sample surface at a 0° view zenith angle. With the 18° foreoptic on the spectrometer, the diameter of the field of view at the sample was 28 cm. The sunlight and view angles were chosen to minimize shadowing and to emphasize the fundamental spectral properties of the plant and other materials. We acquired 9–15 spectra of each sample by moving the sensor over the objects to get the average spectra, for comparison with the spectra of the AVIRIS pixels. We calibrated the spectrometer to surface reflectance prior to measurement of each material using a spectralon panel (Kokaly et al., 2003). The spectra collected in the field campaign include live canopy of each dominant species of trees, shrubs and herbaceous, dead plant materials, charred wood, bare soils and rocks. The original spectral records were then summarized for each material to create standard spectral curves, and were subsequently convolved to the 2002 AVIRIS data set using the band centers and full-width-half-maxima (FWHM) for that flight line (Fig. 2A, B).

2.4. AVIRIS data collection and pre-processing

High-altitude AVIRIS radiance data (Green et al., 1998) were acquired with an ER-2 aircraft at an altitude of approximately 20 km by NASA's Jet Propulsion Laboratory (JPL) on October 15, 2002 beginning at 18:34 UTC (12:34 MT) over the Colorado Front Range, covering the central part of the Pike National Forest. The AVIRIS mission transected a small piece of prairie grassland landscape, with a wildland/urban interface, to the ponderosa pine/Douglas-fir forest in the Front Range region, crossing Douglas County, Jefferson County, Park County, and Teller County of Colorado. The flight followed the Front Range from north to south, providing approximate 10.5 km swath and 53 km length of flight lines in 224 spectral channels with a nominal FWHM of 10 nm from 370 to 2510 nm. Five overlapping flightlines were collected. There were shadow effects and patches of snow at the higher elevation line (r18), with slight haze over its southwest portion, so we excluded this flightline from our image analysis.

Vegetation types seen in the images were predominantly ponderosa pine/Douglas-fir forest, juniper woodland and grassland. Due to the frequent wildfire in the region, fire footprints of different ages were included in the data collection area. The flight included geomorphic features of mountain range, basin, and low basin rim, rising from the Great Plains to the Rocky Mountains.

The original JPL AVIRIS datasets, which contain four flight lines at a pixel resolution of 14.6–17.0 m, were initially georectified with an onboard global positioning-inertial navigation system (GPS-INS) by the data provider using JPL standard techniques (Green et al., 1998). We registered the AVIRIS scenes to an orthorectified airphoto mosaic, transformed them using triangulation, resampled using nearest-neighbor resampling, and then created a mosaic of four flightlines at a pixel resolution of 15 m. We then atmospherically corrected the resampled AVIRIS datasets, and converted the data to reflectance using the High-Accuracy ATmospheric Correction for Hyperspectral Data (HATCH) algorithm (Goetz et al., 2003). In the HATCH process, two water vapor bands, 0.86–1.05 and 1.05–1.25 were used in calibration. Even after the calibration, there were still atmospheric effects in a group of bands. We selected a subset of 190 bands from the registered reflectance image to remove bands with strong water absorption features in the shortwave infrared (SWIR), bands with poor signal-to-noise ratio in the blue end of the visible spectrum, and the SWIR beyond 2450 nm wavelength.

2.5. Spectral mixture analysis and mapping

Many approaches have been devised to analyze the fractional cover of PV, NPV, and bare soil, all applied mainly in arid and semi-arid regions. The visible and infrared spectral regions (400–1300 nm) used to detect green vegetation do not easily separate the fractions of NPV and bare soil, but the short-wave

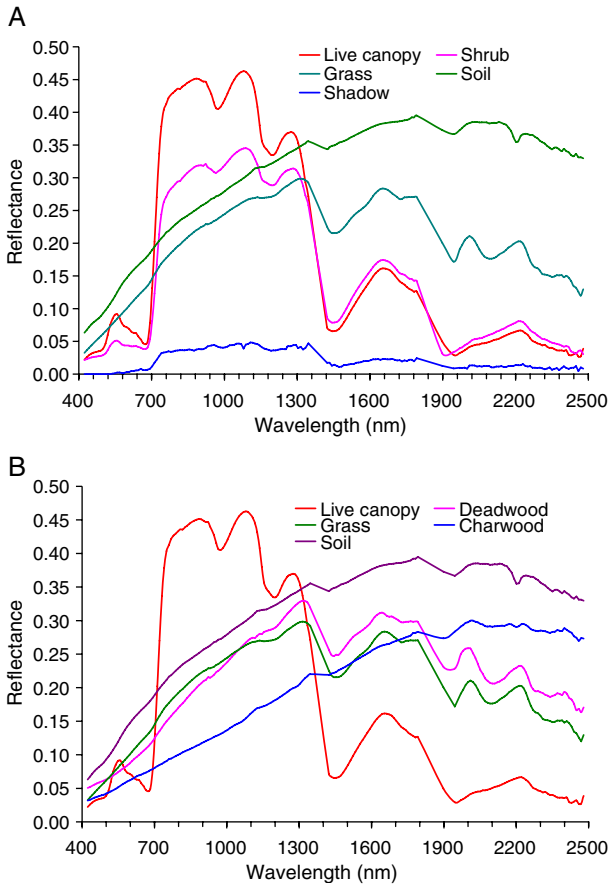

Fig. 2. (A) Field spectra for a conifer forest showing the separation of PV (live canopy, shrub, live grass), NPV (deadwood, senescent grass, litter), and bare soil. (B) Field spectra for a burned forest showing the separation of PV (live canopy, shrub, live grass), NPV (senescent grass, litter, deadwood), and bare soil (soil, char wood).

infrared (SWIR) of the AVIRIS spectrum is promising in isolating the unique spectral features of those surface materials (Asner & Heidebrecht, 2003; Roberts et al., 1993, 1998). Based on field spectroscopy and AVIRIS data, we undertook a spectral mixture analysis (SMA) to decompose image pixels into sub-pixel fractions of PV, NPV, and bare soil. SMA is a technique based on modeling image spectra as the linear combination of endmembers; SMA has been used to derive the fractional contribution of endmember materials to image spectra in a wide variety of applications (e.g., Asner et al., 1998; Kokaly et al., 2003). This approach assumes that image pixels contain endmember cover fractions that can be linearly summarized, where the sub-pixel cover fractions of each mappable land-cover endmember may be PV, NPV, or bare soil. Thus, SMA 'unmixes' the mixed pixel determining the fractions of each spectral endmember that combine to produce the mixed pixel's spectral signature. Assuming linear mixing, i.e., the spatial fractions equal the spectral fractions, these fractions are considered to be the areal fractions. Because there are a number of endmember combinations that can produce a particular spectral signal, a wide range of numerically acceptable unmixing results for any image pixel are possible (Asner et al., 1998). SMA techniques that use endmember reflectance ''bundles'' account for this natural variability (Bateson et al., 2000).

We used the AVIRIS mosaic apparent reflectance data to analyze the spectral mixtures of PV, NPV, and bare soil, using ENVI 4.1 (Research System Inc., Boulder, CO, USA) based on the methods and procedures described by Roberts et al. (1993, 1998) and Asner and Heidebrecht (2003). The selection of a reflectance endmember bundle (Bateson et al., 2000) for spectral mixture analysis is critical, and often difficult for accurately estimating sub-pixel fractions. These endmembers are usually either from image spectra or from a spectral library built from field measurements. In dense and undisturbed forest areas, image spectra are more representative of pure PV than the field spectra measured at the branch level, which usually do not fit the spectral properties of the entire canopy well. Therefore, we used our field spectra from 14 plot samples of dense green vegetation located on a relatively flat surface (to eliminate shadow) as training areas to generate image spectra of the PV endmember. We used the average field spectra of senescent vegetation and bare soil collected in the areas to represent spectra of NPV and bare soil respectively. We chose to use the field spectra because pure pixels of NPV and soil are rarely available in images of forest areas, and field spectra of NPV and soil are highly scalable (Bateson et al., 2000; Roberts et al., 1998). Using the reference spectra of the three components, we analyzed the spectral mixtures and generated fraction images of PV, NPV, and bare soil by modeling each pixel as a combination of three endmember bundles (Bateson et al., 2000). Within the linear spectral mixture analysis procedure, we created one fraction map for each endmember bundle. The fraction maps assign a value for each pixel indicating what percentage of the pixel can be modeled by that endmember bundle. For example, the NPV fraction maps have high values for those areas covered predominantly by NPV, whereas the same pixels would have low values on the green vegetation fraction map. Finally, the unmixing procedure identified the subpixel abundance of PV, NPV, or soil in each pixel in the study areas.

We calculated the coefficients of determination to examine the correlation between the hyperspectral estimates of forest component fractions and field measured fractional cover. Field data came from the transect sampling within the image coverage, and the AVIRIS estimates of PV, NPV, and bare soil were

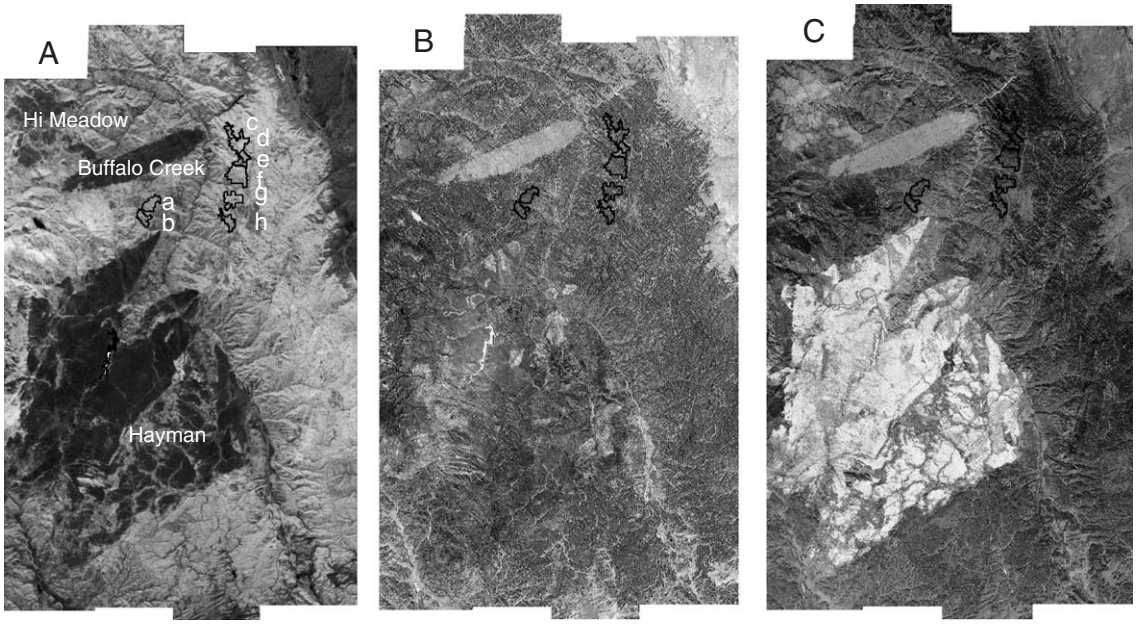

Fig. 3. Images of fractional cover of each forest component in the upper South Platte (Grey scale). Darker colors represent lower fraction, and values range from 0–1. A) PV; B) NPV; C) bare soil. The polygons represent US Forest Service treatment areas, they are: a — Dell Gulch, b — Kelsey Gulch, c — Bennett Mountain, d — Russell Ridge pre-treatment, e — Russell Ridge Treated, f — Nighthawk, g — Noddle Head, h — Bear Mountain. The extension of the Hayman Fire, the Buffalo Creek Fire, and the Hi Meadow Fire are clearly seen on the images.

derived from 9-pixel blocks centered at corresponding field sites. The correlation was applied to all three types of fractional cover.

These analyses provided us maps of abundance of each fractional cover type with confidence from field validation. We spatially summarized the fractional cover of forest components over US Forest Service fuel treatment areas and recently burned areas located within the image and compared the ratio of these components among the areas using the ArcGIS spatial analysis module (ESRI, Redland, CA, USA).

3. Results and discussion

3.1. Validation of AVIRIS derived maps of fractional cover

Subpixel level fractional cover estimates of PV, NPV, and bare soil were derived from high altitude AVIRIS reflectance data, and map layers of fractional cover for these three components were created (Fig. 3). An accuracy assessment based on a 34 field transects dataset yielded coefficients of determination of 73.5%, 40.3%, and 77.6% for PV, NPV, and soil respectively in terms of fractional cover. Thus, we were able to describe over 70% of the variance for PV and soil, but much less of the variance for NPV. PV fractions from AVIRIS were highly correlated with field green vegetation measurements ($r^2=0.73$, $p<0.01$), showing the capacity of AVIRIS data for detecting sub-pixel level photosynthetic vegetation in forest areas despite the complex structure compared to shrubland and grassland (Fig. 4). The fractional cover of bare soil derived from the AVIRIS image was also highly correlated with the ground measurements (Fig. 4C; $r^2=0.78$, $p<0.01$). Estimates of bare soil fractional cover were relatively more accurate in sparse forests and openings ($r^2=0.91$, $p<0.001$) than in dense forest ($r^2=0.63$, $p<0.01$). High fractions of bare soil were found in

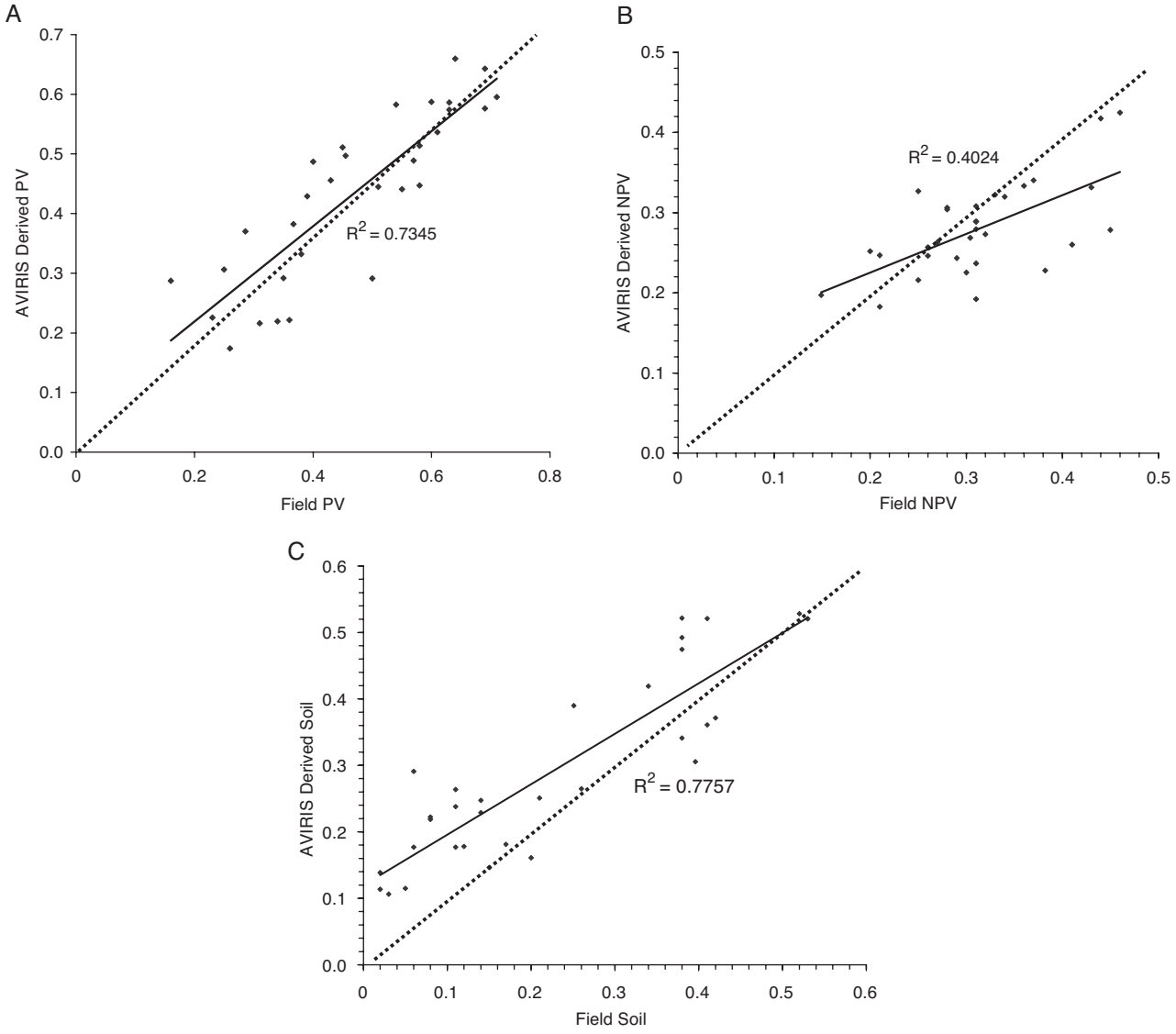

Fig. 4. Comparison between hyperspectral image spectral mixture analysis derived fractional covers of forest components and field measured fractional cover. The dotted are 1:1 lines. A) PV; B) NPV; C) bare soil.

recently burned areas and near residential areas (Fig. 4C). Sub-pixel NPV fractions from the AVIRIS derived image were validated by field NPV measurements, with a significant relationship that explained less of the variation than PV and bare soil fractions (Fig. 4B; $r^2 = 0.40$, $p < 0.05$).

There are several factors that may have contributed to the low correlations between AVIRIS-derived NPV and the field estimates. First, dead branches and partially scorched tree crowns that were recorded as NPV in the field were apparently not fully detectable by the AVIRIS sensor. The method used to estimate PV and NPV in the field is likely to underestimate NPV and overestimate PV, since it assigns entire live crown area to PV (even though some of this crown comprises non-photosynthetic branches and twigs). Second, some transects were sampled in earlier stages of the growing season and therefore grasses were recorded as PV, whereas they were identified on AVIRIS data as NPV. Third, as NPV is a complex bundle of non-photosynthetic canopy, dead wood, dry grasses, and litter; it was more challenging to select representative endmember bundles for NPV than other types. Therefore, further tests on both field fractional cover measurements and endmember selection in the SMA process will likely improve hyperspectral estimate of the fraction.

Photogrammetric shade was treated as an endmember in some SMA cases, especially in multiple endmember spectral mixture analysis (MESMA), in PV–NPV–shade or vegetation–soil–shade models (Roberts et al., 1998). We used a three endmember PV–NPV–soil model and excluded shade for several reasons. First, SMA has been successful with up to three endmember models so far. Running a four-endmember model was expected to result in unacceptable fraction errors (Asner et al., 1998; Roberts et al., 1993). In assessing fire risks, a PV–NPV–soil is more appropriate than any three endmember model with shade. Second, photogrammetric shade was reduced after topographic correction by JPL (Green et al., 1998) and we had excluded the flightline (r18) with most shade in our analysis. Finally, our validation results suggested that shade was unlikely a major source of error in our case.

Though AVIRIS imagery has promise for discriminating various materials in the canopy layer and within gaps in relatively sparse forests, the sensor, as with any passive sensors, cannot penetrate through tree crowns and detect spectral signatures directly under tree canopy. Therefore, the denser the forest is, the more the understory signatures are missed by AVIRIS, and the lower likely accuracy (Fig. 4). When we examine the validation samples, we find that those sites that have a low fraction of PV and a high fraction of soil have the highest agreement between AVIRIS and field data, even for NPV, while most of deviations were related to areas with a large PV fraction and small soil fraction. During our sampling, most of the understory vegetation was senescent, and therefore, did not have much contribution to PV, such that AVIRIS-sensed PV was similar to field estimates. In summary, given appropriate timing of study, AVIRIS is capable of isolating the PV fraction in coniferous forests with a deciduous understory, but has limitation with NPV. Further tests may involve combining AVIRIS and active sensor such as Lidar (Lefsky et al., 2002).

3.2. Spatial patterns of PV, NPV, and soil fractions

Throughout the South Platte study area, PV fractions were dominant (48.7%), followed by NPV (28.8%) and soil (22.5%). Fractional cover estimates of PV, NPV, and bare soil derived from AVIRIS reflectance measurements varied substantially across the study region (Fig. 3.). There were high fractions of PV on north facing slopes and in old growth forest areas as spatially analyzed against a digital elevation model. For example, in the Nighthawk area (see Fig. 3.) PV covered 62.7% of the north slopes, while the cover dropped to 49.4% on south slopes. This is a common feature of montane Rocky Mountain forests, occurring because of the reduced direct sunlight, lower soil temperatures, lower evaporation, and thus higher soil moisture conditions of north-facing slopes. Bare soil fractions were high in low elevations, on south slopes, and in recently burned areas, particularly those around Cheesman Lake; these patterns likely also occur due to soil moisture. In the late growing season AVIRIS image, most of grasses were senesced, and thus NPV dominated most openings where grasses prevailed (e.g., the elongated Buffalo Creek burn).

PV signatures mainly reflect conifer canopies and some evergreen shrubs under sparse canopy. PV fractions were lower in the pine/grassland ecotone in the northeast and southwest corners compared to forest areas in most of the image (Fig. 3A). Meanwhile, low PV fractions were also found in burned areas of the Hayman and Schoonover Fires, the Buffalo Creek Fire, and the Hi Meadow Fire. Another apparently low PV area was found just east of the Noddle Head and Bear Mountain treatment areas, where insect infestation had caused about 50% mortality of Douglas-fir. The fraction of PV is normally close to live canopy cover in vegetation that has a simple vertical structure, such as grassland and desert shrub (Asner & Heidebrecht, 2003). However, in multi-layer forest sites, the PV fraction reflects live tree canopy and understory live shrubs, seedlings, and live grasses. We found that the PV fraction was on average 11.7% higher than canopy cover in the woodland sites with 40% or less canopy cover, presumably contributed by understory vegetation. PV fractions in shrublands and grassland/meadow sites varied from 16.7–47.5%, showing the proportion of shrub and grass foliage still active in mid-October in these openings.

There was 0–12% of bare soil detected in dense forest with over 60% canopy cover, but there was no significant trend of increasing fraction of bare soil with decreasing canopy cover in woodland and openings. Therefore, fraction of bare soil is more likely a function of ecosystem disturbances and secondary succession than forest structure itself under similar climatic conditions.

NPV signatures reflect dead wood, litter, and senescent grasses and deciduous shrubs. These include volatile surface fuels and are thus extremely important for remotely sensed fire risk assessment when combined with live vegetation. The areas with high NPV fractions included forests that had been recently burned at low to medium severity, and forests after insect infestation. Fire has a mixed effect on NPV fractions: it turns live tree crowns (including those lethally scorched but not burned) into NPV, offsetting the consumption of litter and

woody debris (NPV), and it exposes bare soil. In addition, areas with recent mechanical thinning (mastication or partial biomass removal) showed a high fraction of NPV, likely because of a larger amount of woody debris and senescent grasses on the ground surface, and a reduced number of seedlings and shrubs because of the treatment. Dense grassland and shrubland also showed high NPV, again due to the season of the AVIRIS overflight.

Although the fractional cover values derived from the AVIRIS image and field survey fit well in most cases, there were noticeably greater errors in areas of high PV and low NPV/soil. The AVIRIS spectral mixture algorithm appeared to underestimate the fractional cover of PV at very high values. Two reasons may have led to this. First, branches and twigs of live tree crowns exposed to AVIRIS sensor were measured as PV in the field, but are spectrally more like NPV. Second, understory live shrubs and herbaceous were counted as PV in the field but may have been overlaid with tree crowns, and therefore can't be detected by AVIRIS sensor. Nevertheless, as AVIRIS cannot penetrate through forest canopy, it tends to ignore understory materials in dense forests. NPV was generally underestimated by SMA (Fig. 4B); this was especially true with high NPV fractions (i.e., over 30%). Our results demonstrate the limitation of AVIRIS in detecting surface materials that are important for fire behavior. Finally, soil tended to be overestimated by SMA at very low fractions (i.e., less than 10%) but generally fitted well with field measurements.

3.3. Effect of disturbances on fractional covers

There were regional trends and major differences among experimental areas in the fractional cover of forest components (Fig. 3). First, there was a high fraction of PV east of Hayman burned area and low fraction of PV in burned areas. Second, in the Hayman fire area, PV fractions tended to decline with increase in burn severity, while bare soil tended to increase with burn severity. We summarized the fractional covers against a Landsat derived map of Hayman fire burn severity provided by Burned Area Emergency Stabilization and Rehabilitation (BAER) (BAER Report, Hayman Fire, 2002, http://www.fs.fed.us/r2/psicc/hayres/), resulting in 37.8%, 42.2%, and 56.9% of bare soil fractions, 25.5%, 31.6%, and 28.9% of NPV, and 36.7%, 26.2%, and 13.2% of PV over areas with low, moderate, and high burn severity respectively. Interestingly, the highest NPV fractions (31.6%) appeared in the areas with moderate burn severity, probably reflecting the large number of standing dead and downed trees, including trees with scorched foliage (Omi & Martinson, 2002) and less consumption of litter and duff. In the Hi Meadow burned area (2000 fire, see Fig. 3), PV cover was the lowest (29.9%) among the nine areas studied, while bare soil cover was the highest (37.8%). This indicates the effect of severe wildfire on reducing ground vegetation cover; because of the reduced ground cover, it also indicates a high risk of soil erosion for at least two years following fire (Pierce et al., 2004). Third, there were apparent differences in all three fractions between recent USFS fuel treatment areas and untreated areas.

As part of the national fuel reduction plan, mechanical thinning, which mainly targets small diameter trees, was conducted in early 2002 in a 70-acre area (Russell Ridge Treated, Fig. 3). The effects of the treatment, though modest, were clearly seen on fraction images, with an 11.7% decrease in PV, a 7.2% inzcrease in NPV, and a 4.5% increase in bare soil compared with nearby untreated forests (Russell Ridge) (Fig. 5). The results of the fuel treatment identified from the AVIRIS data were similar to what we expected: the decrease of PV fraction reflected thinned canopy without small diameter trees, while increases of NPV and soil likely occurred because downed wood remained on the ground and new gaps were created by the thinning. This demonstrates that image spectroscopy can be used to assess and compare fuel types and fire risks following different fuel treatment scenarios.

Generally, large fractions of NPV favor rapid fire spread and crowning, while bare soil retards fire spread in most cases. The role of PV in fire risk is more complex. Dense forest with a large amount of fuels below the canopy ("ladder fuels", reaching from ground to canopy) reflect a high fire risk, however, forests with low PV fraction are normally drier and contain more 1- and 10-h fuels (Brown et al., 1982) that make wildfire easy to start. The increase in NPV fraction due to various disturbances may cause a higher risk of surface fire. Our study demonstrated that the fractional cover of PV, NPV, and bare soil are extremely spatially heterogeneous in both burned and unburned forests, and that these fractions are remotely measurable. Discrimination of PV, NPV, and bare soil fractions provide important inputs for fire risk analysis, but additional information such as surface fuel loading, species composition, and amounts of ladder fuel are needed to achieve the most effective fuel modeling.

4. Conclusions

Our study demonstrated that spectral mixture analysis of AVIRIS imagery provides estimates of photosynthetic vegetation, non-photosynthetic vegetation, and soil that are highly

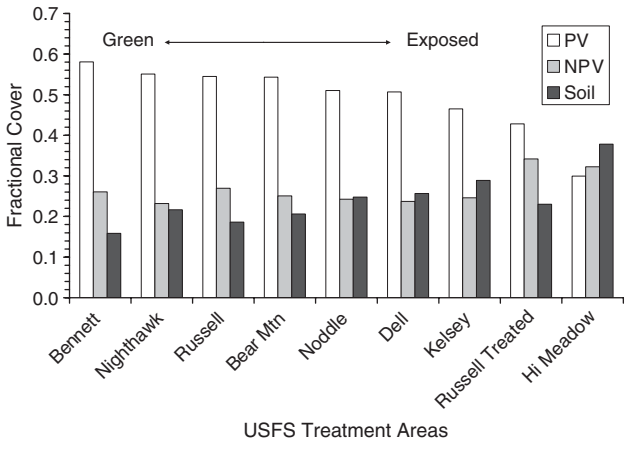

Fig. 5. Distribution of fractional covers of photosynthetic vegetation, non-photosynthetic vegetation, and bare soil among USFS fuel treatment areas, showing the effect of microclimate, disturbance, and fuel treatment on fractions of the forest components. See Fig. 1. for the location of the areas.

correlated with field transect measurements of green vegetation, dead plant materials, and soil fractions. AVIRIS derived fractional land cover can thus serve as a useful indicator of forest fuel condition. Meanwhile, as NPV is a complex bundle of non-photosynthetic canopy, dead wood, dry grasses, and litter, further tests on both field fractional cover measurements and endmember selection in SMA process is needed to improve hyperspectral estimates for this fraction.

Our study also demonstrated that the fractional cover of PV, NPV, and bare soil are extremely spatially heterogeneous in both burned and unburned forests of the Colorado Front Range. The AVIRIS derived maps indicate that recent mechanical thinning generally leads to a decrease of PV and increases in NPV and soil. Fire has a complex impact on the fractions: it reduces PV and creates new bare ground (soil), while light to moderate burns are related to a higher fraction of NPV.

Maps derived from hyperspectral images permit the evaluation of fuel treatment efforts by managers, an otherwise extremely labor intensive process. One of the most interesting and poorly understood aspects of wildfires is the ratio of live and dead vegetation remaining following a fire. Our study provided an opportunity to improve this understanding. With accurate estimates of the spatial distribution of each fuel component, our results could greatly improve regional land cover estimates, fire behavior predictions, and carbon assessment efforts. Meanwhile, a more effective fire risk assessment could be achieved by assessing and adjusting current fuel treatments with the information provided here. Hyperspectral remote sensing may be a viable approach to estimate forest fuel condition at the regional level in coniferous forests across western US, given an increasing availability of airborne (e.g., CASI, HyMap) and spaceborne (e.g., Hyperion) instruments for research and management.

Acknowledgements

This study was supported by the NASA Carbon Cycle Science program (NRA-00-OES-08) and by the Joint Fire Sciences Program (Project 01-1-3-22). We thank our field crew Andrew Schaefer, Paul Cada, Dayle Funka, and Claire Ojima for collecting ground-truthing data, and Chris Bennett for his technical support. We also thank U.S. Forest Service professionals Fred Patton, Steve Culver, and Barry Johnston of the Pike National Forest for their expertise and assistance.

References

Andersen, H. -E., McGaughey, R. J., & Reutebuch, S. E. (2005). Estimating forest canopy fuel parameters using LIDAR data. *Remote Sensing of Environment*, *94*(4), 441−449.

Asner, G. P., & Heidebrecht, K. B. (2003). Imaging spectroscopy for desertification studies: Comparing AVIRIS and EO-1 Hyperion in Argentina drylands. *IEEE Transactions on Geoscience and Remote Sensing*, *41*(6), 1283−1296.

Asner, G. P., Wessman, C. A., & Schimel, D. S. (1998). Heterogeneity of savanna canopy structure and function from imaging spectrometry and inverse modeling. *Ecological Applications*, *8*(4), 1022−1036.

Baker, W. L. (1992). Effects of settlement and fire suppression on landscape structure. *Ecology*, *73*, 1879−1887.

Bateson, C. A., Asner, G. P., & Wessman, C. A. (2000). Endmember bundles: A new approach to incorporating endmember. *IEEE Transactions on Geoscience and Remote Sensing*, *38*(2), 1083−1094.

Bergen, K., Colwell, J., & Sapio, F. (2000). Remote sensing and forestry: Collaborative implementation for a new century of forest information solutions. *Journal of Forestry*, *98*(6), 4−9.

Brown, J. K., Oberheu, R. D., & Johnston, C. M. (1982). Handbook for inventorying surface fuels and biomass in the interior west. *USDA Forest Service General Technical Report INT-129.* Fort Collins: USDA Forest Service.

Brown, T. J., Hall, B. L., & Westerling, A. L. (2004). The impact of twenty-first century climate change on wildland fire danger in the western United States: An applications perspective. *Climatic Change*, *62*(1–3), 365−388.

Burgan, R. E., Klaver, R. W., & Klaver, J. M. (1998). Fuel models and fire potential from satellite and surface observations. *International Journal of Wildland Fire*, *8*(3), 159−170.

Dennison, P. E., Roberts, D. A., Thorgusen, S. R., Regelbrugge, J. C., Weise, D., & Lee, C. (2003). Modeling seasonal changes in live fuel moisture and equivalent water thickness using a cumulative water balance index. *Remote Sensing of Environment*, *88*, 442−452.

Dwire, K. A., & Kauffman, J. B. (2003). Fire and riparian ecosystems in landscapes of the western USA. *Forest Ecology and Management*, *178*(1–2), 61−74.

Fornwalt, P. J., Kaufmann, M. R., Huckaby, L. S., Stoker, J. M., & Stohlgren, T. J. (2003). Non-native plant invasions in managed and protected ponderosa pine/Douglas-fir forests of the Colorado Front Range. *Forest Ecology and Management*, *177*(1–3), 515−527.

Fried, J. S., Torn, M. S., & Mills, E. (2004). The impact of climate change on wildfire severity: A regional forecast for northern California. *Climatic Change*, *64*(1–2), 169−191.

Goetz, A. F. H., Kindel, B. C., Ferri, M., & Zheng, Qu (2003). HATCH: results from simulated radiances, AVIRIS and Hyperion. *IEEE Transactions on Geoscience and Remote Sensing*, *41*(6), 1215−1222.

Graham, R. T. (Ed.). (2003). *Hayman Fire Case Study. Ogden, UT: USDA Forest Service Rocky Mountain Research Station. Gen. Tech. Rep. RMRS-GTR-114,* 396 pp.

Green, R. O., Eastwood, M. L., Sarture, C. M., Chrien, T. G., Aronsson, M., Chippendale, B. J., et al. (1998). Imaging spectroscopy and the airborne visible/infrared imaging spectrometer (AVIRIS). *Remote Sensing of Environment*, *65*(3), 227−248.

Hall, S. A., Burke, I. C., Box, D. O., Kaufmann, M. R., & Stoker, J. M. (2005). Estimating stand structure using discrete-return lidar: An example from low density, fire prone ponderosa pine forests. *Forest Ecology and Management*, *208*(1–3), 189−209.

Hyyppa, J., Hyyppa, H., Inkinen, M., Engdahl, M., Linko, S., & Zhu, Y. -H. (2000). Accuracy comparison of various remote sensing data sources in the retrieval of forest stand attributes. *Forest Ecology and Management*, *128*(1–2), 109−120.

Justice, C. O., Giglio, L., Korontzi, S., Owens, J., Morisette, J. T., Roy, D., et al. (2002). The MODIS fire products. *Remote Sensing of Environment*, *83*(1–2), 244−262.

Kaufmann, M. R., Fornwalt, P. J., Huckaby, L. S., & Stoker, J. M. (2001). Cheesman Lake — A historical ponderosa pine landscape guiding restoration in the South Platte Watershed of the Colorado Front Range. *Proceedings RMRS-P-22* (pp. 9−18). Fort Collins, CO: USDA Forest Service, Rocky Mountain Research Station.

Kaufmann, M. R., Huckaby, L., & Gleason, P. (2000). Ponderosa pine in the Colorado Front Range: Long historical fire and tree recruitment intervals and a case for landscape heterogeneity. *Proceedings from the Joint Fire Science Conference and Workshop, June 14–16, 1999, Boise, ID* (pp. 153−160). Moscow, ID: University of Idaho.

Keane, R. E., Arno, S. F., & Brown, J. K. (1990). Simulating cumulative fire effects in ponderosa pine/Douglas-fir forests. *Ecology*, *71*(1), 189−202.

Keeley, J. E., Fotheringham, C. J., & Morais, M. (1999). Reexamining fire suppression impacts on brushland fire regimes. *Science*, *284*(5421), 1829−1832.

Kokaly, R. F., Despain, D. G., Clark, R. N., & Livo, K. E. (2003). Mapping vegetation in Yellowstone National Park using spectral feature analysis of AVIRIS data. *Remote Sensing of Environment*, *84*(3), 437−456.

Laughlin, D. C., Bakker, J. D., Stoddard, M. T., Daniels, M. L., Springer, J. D., Gildar, C. N., et al. (2004). Toward reference conditions: Wildfire effects on flora in an old-growth ponderosa pine forest. *Forest Ecology and Management*, *199*(1), 137−152.

Law, B. E., Sun, O. J., Campbell, J., van Tuyl, S., & Thornton, P. E. (2003). Changes in carbon storage and fluxes in a chronosequence of ponderosa pine. *Global Change Biology*, *9*(4), 510−524.

Lefsky, M. A., Cohen, W. B., Parker, G. G., & Harding, D. J. (2002). Lidar remote sensing for ecosystem studies. *BioScience*, *52*(1), 19−30.

Lynch, A. H., & Wu, W. (2000). Impacts of fire and warming on ecosystem uptake in the boreal forest. *Journal of Climate*, *13*(13), 2334−2338.

Mast, J. N., Veblen, T. T., & Linhart, Y. B. (1998). Disturbance and climatic influences on age structure of ponderosa pine at the pine/grassland ecotone, Colorado Front Range. *Journal of Biogeography*, *25*(4), 743−755.

Miller, C., & Urban, D. L. (2000). Connectivity of forest fuels and surface fire regimes. *Landscape Ecology*, *15*(2), 145−154.

Omi, P., & Martinson, E. (2002). Final report to the Join Fire Science Program on effects of fuels treatment on wildfire severity. *Western Forest Fire Research Center.* Fort Collins, CO: Colorado State University.

Pierce, J. L., Meyer, G. A., & Timothy Jull, A. J. (2004). Fire-induced erosion and millennial-scale climate change in northern ponderosa pine forests. *Nature*, *432*(7013), 87−90.

Roberts, D. A., Dennison, P. E., Gardner, M. E., Hetzel, Y., Ustin, S. L., & Lee, C. T. (2003). Evaluation of the potential of Hyperion for fire danger assessment by comparison to the airborne visible/infrared imaging spectrometer. *IEEE Transactions on, Geoscience and Remote Sensing*, *41* (6), 1297−1310.

Roberts, D. A., Gardner, M., Church, R., Ustin, S., Scheer, G., & Green, R. O. (1998). Mapping chaparral in the Santa Monica Mountains using multiple endmember spectral mixture models. *Remote Sensing of Environment*, *65* (3), 267−279.

Roberts, D. A., Smith, M. O., & Adams, J. B. (1993). Green vegetation, nonphotosynthetic vegetation, and soils in AVIRIS data. *Remote Sensing of Environment*, *44*(2–3), 255−269.

Romme, W. H. (1982). Fire and landscape diversity in subalpine forests of Yellowstone National Park. *Ecological Monographs*, *52*(2), 199−221.

Schoennagel, T., Veblen, T. T., & Romme, W. H. (2004). The interaction of fire, fuels, and climate across Rocky Mountain forests. *BioScience*, *54*(7), 661−676.

Scott, J. H., & Reinhardt, E. D. (2001). Assessing crown fire potential by linking models of surface and crown fire behavior. *USDA Forest Service Rocky Mountain Research Station, Research Paper RP-29.* 59 pp.

Stohlgren, T. J., Falkner, M. B., & Schell, L. D. (1995). A Modified-Whittaker nested vegetation sampling method. *Vegetatio*, *117*, 113−121.

Ustin, S. L., Roberts, D. A., Gamon, J. A., Asner, G. P., & Green, R. O. (2004). Using imaging spectroscopy to study ecosystem processes and properties. *BioScience*, *54*(6), 523−534.

van Wagtendonk, J. W., Root, R. R., & Key, C. H. (2004). Comparison of AVIRIS and Landsat ETM+ detection capabilities for burn severity. *Remote Sensing of Environment*, *92*(3), 397−408.

Veblen, T. T., Kitzberger, T., & Donnegan, J. (2000). Climatic and human influences on fire regimes in ponderosa pine forests in the Colorado Front Range. *Ecological Applications*, *10*, 1178−1195.